AD-A068 164 ROCKWELL INTERNATIONAL THOUSAND OAKS CALIF SCIENCE --ETC F/G 7/4
COMPUTER CONTROLLED ESR.(U)
APR 79 I B GOLDBERG N00014-73-C-0325

UNCLASSIFIED SC549.31FR NL

1 OF 1
AD A068164

END
DATE FILMED
6-79
DDC

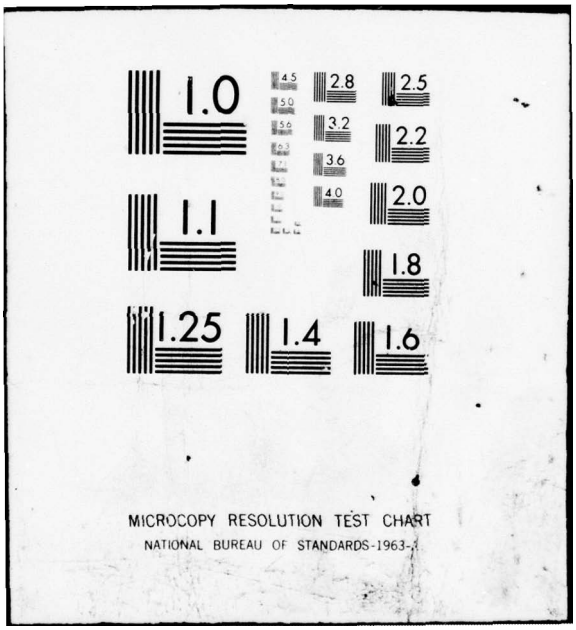
1.0
1.1
1.25
1.4
1.6
1.8
2.0
2.2
2.5
2.8
3.2
3.6
4.0
4.5
5.0
5.6
6.3
7.1
MICROCOPY RESOLUTION TEST CHART
NATIONAL BUREAU OF STANDARDS-1963-A

(12) LEVEL II

10

(11) April 1979

(14) SC549.31FR

(12) 53p.

(6) COMPUTER CONTROLLED ESR

(9) Final Report. 1 Apr 73-30 Nov 78

For period 04/01/73 through 11/30/78

(15) Contract No. N00014-73-C-0325
Project No. NR051-553

Prepared for:

Office of Naval Research
Arlington, Virginia 22217
Attn: Code 472

This work was supported in part by the Office of Naval Research.

Prepared by:

Ira B Goldberg

(10) Ira B. Goldberg

Approved for public release, distribution unlimited.

Rockwell International
Science Center

Unclassified

SECURITY CLASSIFICATION OF THIS PAGE (When Data Entered)

REPORT DOCUMENTATION PAGE		READ INSTRUCTIONS BEFORE COMPLETING FORM
1. REPORT NUMBER	2. GOVT ACCESSION NO.	3. RECIPIENT'S CATALOG NUMBER
4. TITLE (and Subtitle) COMPUTER CONTROLLED ESR Final Report		5. TYPE OF REPORT & PERIOD COVERED Final Report 6. PERFORMING ORG. REPORT NUMBER 04/01/73 - 11/30/78
7. AUTHOR(s) Ira B. Goldberg		8. CONTRACT OR GRANT NUMBER(s) N00014-73-C-0325
9. PERFORMING ORGANIZATION NAME AND ADDRESS Science Center Rockwell International Thousand Oaks, CA 91360		10. PROGRAM ELEMENT, PROJECT, TASK AREA & WORK UNIT NUMBERS NR051-553
11. CONTROLLING OFFICE NAME AND ADDRESS Materials Sciences Division Office of Naval Research Arlington, VA 22217		12. REPORT DATE April 1, 1979 13. NUMBER OF PAGES 50
14. MONITORING AGENCY NAME & ADDRESS (if different from Controlling Office) Office of Naval Research - Branch Office 1030 East Green Street Pasadena, CA 91106		15. SECURITY CLASS. (of this report) Unclassified 15a. DECLASSIFICATION/DOWNGRADING SCHEDULE

16. DISTRIBUTION STATEMENT (of this Report)

Approved for public release, distribution unlimited.

17. DISTRIBUTION STATEMENT (of the abstract entered in Block 20, if different from Report)

18. SUPPLEMENTARY NOTES

19. KEY WORDS (Continue on reverse side if necessary and identify by block number)

Electron Spin Resonance (ESR)
Electron Paramagnetic Resonance (EPR)
Computer, Laboratory
Organic Free Radicals
Radical Ions
Perfluoroammonium salts
Analytical Methods
Thianthrene
Integration

20. ABSTRACT (Continue on reverse side if necessary and identify by block number)

Research in the development and application of a computer-controlled EPR spectrometer is described. The limitation and advantages of the computer are discussed in conjunction with studies on unstable organic radical ions, precision of g-factor and hyperfine splitting, measurements, line-shape analysis and determination of transient lifetimes. The computer permitted considerably greater precision in analytical measurements allowing accuracies of ±1%. Various data processing algorithms are also briefly discussed.

DD FORM 1 JAN 73 1473 EDITION OF 1 NOV 65 IS OBSOLETE

Unclassified

SECURITY CLASSIFICATION OF THIS PAGE (When Data Entered)

TABLE OF CONTENTS

1.0 INTRODUCTION

The objective of this work has been to develop and utilize an interactive laboratory computer interface to facilitate EPR studies of transient species and to improve the analytical capability of EPR. To date, we have employed and are continuing to employ the interactive computer-EPR system in a variety of problems. This has permitted the evaluation of the interactive computer in the EPR laboratory, as well as provided a unique capability in which many difficult experiments are being carried. out.

The basic EPR-computer interface has been described in Technical Report 1 which has been published.[1] This apparatus was utilized in studies of stable and unstable radical anions of tertiary-butyl naphthalene including the observation of valence bond isomerization[2-5] (Technical Reports 2, 4, 5, and 6), studies of triplet states of thianthrene derivatives[6] (Technical Report 3), in the development of analytical techniques for EPR[7-9] (Technical Reports 7, 8, and 9), and in the study of the formation of NF_4^+ salts by UV radition of NF_3, F_2 and either AsF_5 or BF_3[10] (Technical Report 10).

Additional work involved studies on electrogenerated olefinic radical anions, F-atom chemical reactions in the gas phase, and improvements in the EPR computer interface and data processing

The developments made on this contract also affected work in other areas. These include understanding the lunar regolith evolution by measuring the amount of spherical Fe° in lunar fines, developing diagnostics for the O_2-I energy transfer laser by determining accurate $O_2(^1\Delta g)$ concentrations,

measuring the purity of chromium compounds formed in nuclear reactor systems, and extending the range of measurements in gas phase flow reactors.

2.0 EPR COMPUTER-SYSTEM

The EPR-computer interface that was developed during the early stages of this contract was described in detail in Technical Report 1 and in Ref. 1. A reprint of this report is given in Appendix 1. Initially, a Fortran program was used with the original PDP-8/m computer system. Drawbacks in this arrangement were that the Fortran program consumed too much of core when a large data set was recorded. In order to rectify this situation, several assembly language programs were written for specific tasks. While this worked quite well, and enabled accumulation of up to 4000 double-precision data points, difficulties arose when the program needed to be modified to incorporate a different task. For example, it was necessary to rewrite the program in order to include triggering a flash lamp and sensing whether the lamp fired. At that point we realized that with all of the numerous ways in which EPR can be used, if certain experiments were altered, then for each new experiment extensive revisions of the program would be required. This conclusion is equivalent to that of Phillips, Burke, and Wilson.[11]

Our own solution to this problem was to convert our program to a series of user-defined assembly language routines which could be coupled by a BASIC program. These subroutines are listed in Table I with their function in the EPR experiment.

TABLE I

USER FUNCTIONS FOR THE EPR OPERATING SYSTEM

DIS (X,Y)	Display X and Y coordinates of a data point.
CLR (D)	Clear display screen.
CLK (T)	Set up real-time clock, T is the number of clock periods (at present 0.2 ms/unit)
CLW (D)	Wait for clock overflow.
ADC (N)	Get value from channel N on the analog to digital converter.
DAC (W)	Set digital to analog converter to value W.
MAG (Z)	Set magnet control relay by Z (Ø = stop scan, 1 = upfield scan, 2 = downfield scan)
MGW (D)	Wait for magnet scan to stop at lowfield limit.
TRG (D)	Trigger auxiliary pulse (flash, electrochemical, etc.).
EPR (X,Y,T,N)	Rapid scan EPR data acquisition (in progress).
TSC (Y,N)	Time dependent data acquisition (in progress).
BRI (M1)	Bit reverse
BRV (M2)	Bit reverse index M
MOD (M1, M2)	Return N modulus M.

The basic program "ESRLAB" links these subroutines to form a data acquisition package which permits a minimum time between points of 0.2 ms. In addition, the files are automatically sequenced, such that files of 512 data points can be collected every 10s. The duration beween file collection is primarily the result of transferring data to disk.

Not yet completed, are longer subroutines EPR (X,Y,T,N) which will permit more rapid data acquisition when we obtain a faster clock, and TSC (X,N) which will permit recording shorter transients. These will be completed as needed.

One of the features that this system permits is the use of dual-channel recording even at fairly rapid sweep rates, such that field calibrations can be run with the transient species. This permits accurate g-factors and hyperfine splittings to be determined.

3.0 STUDIES OF UNSTABLE ORGANIC RADICAL IONS

Numerous difficulties exist in studies of organic radical ions which are not sufficiently stable such that EPR spectra can be obtained at slow scan rates. Of primary importance is maintaining uniform concentration throughout the spectrum in order to carry out proper analysis. Linear scan rates are also difficult to obtain at fast sweeps, and if auxiliary coils are used to sweep the magnetic field, then poor field homogeneity results, causing distorted lineshapes and poor spectral resolution.[12,13] An additional drawback of auxiliary coils is that dual cavity operation is not possible. This precludes obtaining accurate g-factors which is important in making structural assignments.

Many of these problems can be overcome if the computer can be used to control the magnet functions where rapid sweeps can be used. For example, a

comparison of the performance between auxiliary coils and using the computer-interfaced spectrometer is given in Table II.

The ability to use dual cavity techniques allows the starting point of each scan to be determined by a reference signal (described in detail in Ref. 1), whereas there is always hystersis in the auxiliary coil sweep, and the dual cavity provides a means to measure the g-factor.

TABLE II

COMPARISON OF THE APPLICATION OF HELMHOLTZ COILS VS COMPUTER-CONTROLLED EPR FOR RAPID FIELD SWEEP

	Computer-Controlled EPR	Auxiliary Coils[1]
Maximum Scan Rate	200 G/s	250 G/s
Homogeneity at 20 G Excursion (Over Sample)[3]	<20 mG	500 mG
Linearity of 50 G/s[4]	0.05%	2%[2]
Reproducibility of Starting Point of Sweep Over 128 Repetitions	10 mG	250 mG
Reference Triggering From Dual Cavity and Internal Field Calibration	Usable	Not Usable

1. Coils as described in Ref. 10.
2. Note that at higher scan rates and excursions the linearity and homogeneity would decrease, whereas it woould not affected utilizing the computer system.
3. Estimated.
4. Coefficient of second-order term in the least-squares analysis of data.

3.1 Application to 1,8-di-tert-butyl Substituted Naphthalene Anions

The role of the computer in the study of the radical anions of 1,3,8-tri-tert-butylnaphthalene (TB3N) 1,3,6,8-tetra-tert-butylnaphthalene anions were two-fold. Most important was to be able to signal average spectra repeated at sweep rates from 2 to 50 G/s over a range of 20 G, with exceptionally high resolution. The necessity of rapid sweep rates in these experiments arises because of the short lifetime (400 s at -70°C to < 30 s at +20°C) of these radical ions. To obtain reasonable spectra, the scan duration must be significantly shorter than the lifetime. Also, the amplitudes of the ^{13}C hyperfine lines are only a few percent of the major proton lines, so that the signal-to-noise ratio is relatively low. Using the techniques described below, ^{13}C lines were observed (Fig. 1) at temperatures up to 10°C (half life ~ 80 s).

The sampling requirements are that 2000 data points be collected at increments as small as 0.2 ms, and the reproducibility of the magnetic field must be within ±0.005 G per point. This was achieved by the above techniques.

Using both the proton and ^{13}C hyperfine splittings (hfs) of TB4N and the proton hfs of TB3N , we were able to establish that the angle of intercept of the plane of the 1, 2, and 9 atoms (or 7, 8, and 9 atoms) with the median plane of the molecule is 23±3°. We also found that the molecule was significantly distorted in regions opposite to the 1 and 8 positions although the actual positions could not be assigned. Recently, a crystal of 1,3,6,8-tetra-tert-butylnaphthalene suitable for X-ray analysis was prepared, which indicated that the intercept angle is 21°,[14] and that there is slight

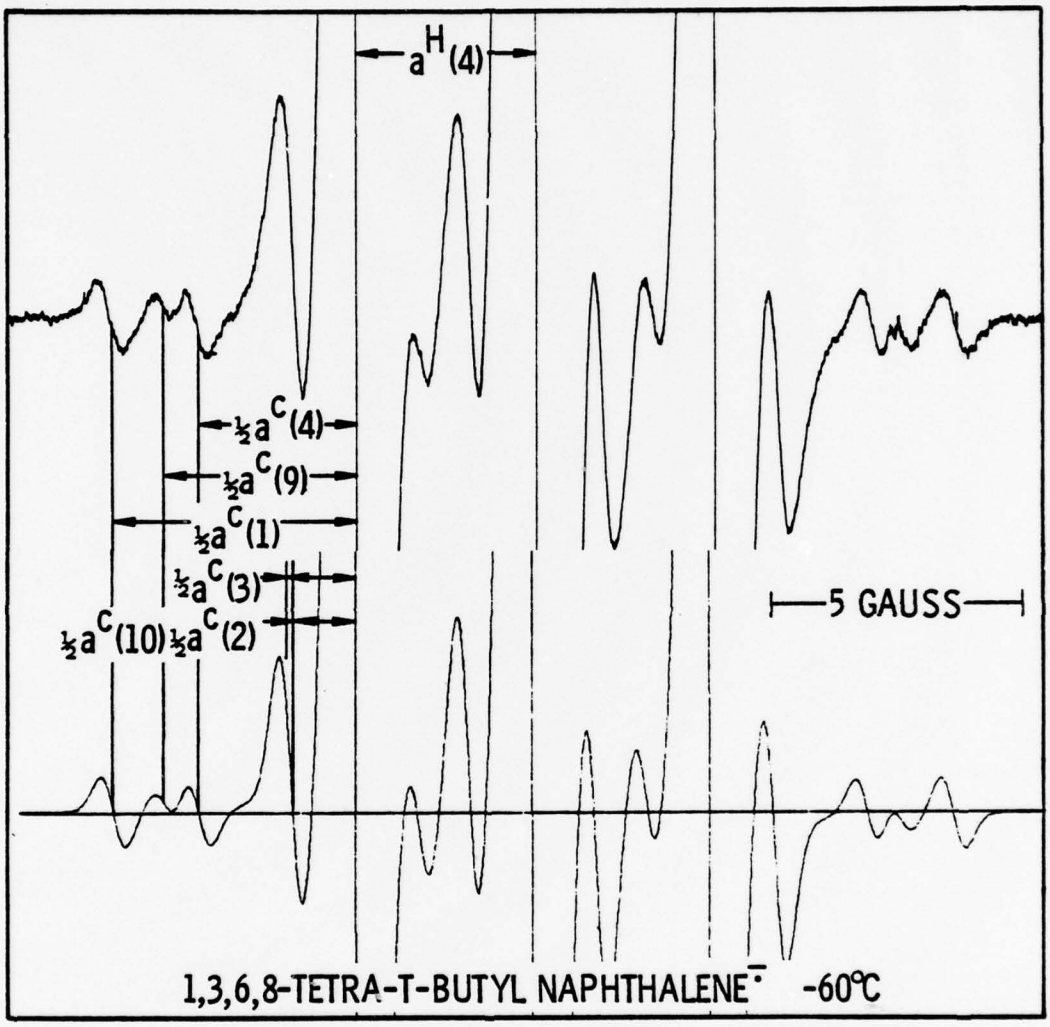

Figure 1

^{13}C Satellite lines of 1,3,6,8-tetra-tert-butynaphthalene anion at -60° (upper); simulation of EPR Spectrum based on assigned splitting constants (see ref. 2).

non-planarity at the 4- and 5-positions. The success of the EPR analysis depended upon the high resolution and relative intensities of hyperfine splittings from protons and naturally abundant ^{13}C.

3.2 Structure and Dynamics of Ion Pairing

During the studies on the 1,8-di-tert-butylnaphthalene anions, the relative amplitudes of the lines were found to be non-integral. Two possibilities could account for this process: (1) a relaxation process, such as the alternating linewidth effect[15] could occur due to 180° out-of-phase motion of the carbon atoms at the 1- and 8-positions or motion of the alkali metal cation in the vicinity of the anion, either of which could cause a modulation of the hyperfine splittings and thus a relaxation process, or (2) a static system in which the hyperfine splittings of the 4 and 5 protons become slightly different as a function of temperature.

In order to discern whether a dynamic or static process was taking place, it was necessary to look for inflections in derivatives of spectra recorded in Fig. 2 since the spectra changed slowly with temperature. Up to 256 sweeps were averaged. It was found that the center line of the spectrum could be accurately fit by a Lorentzian lineshape (dominated by T_2 relaxation) whereas the outside lines were nearly Gaussian (dominated by unresolved splittings from the tert-butyl groups). This unequivocally defined the process as resulting from an alternating linewidth relaxation. Changing the counter ion or solvent also changed the temperture dependence of the spectra, thus the alternating linewidth was attributed to perturbations in the spin

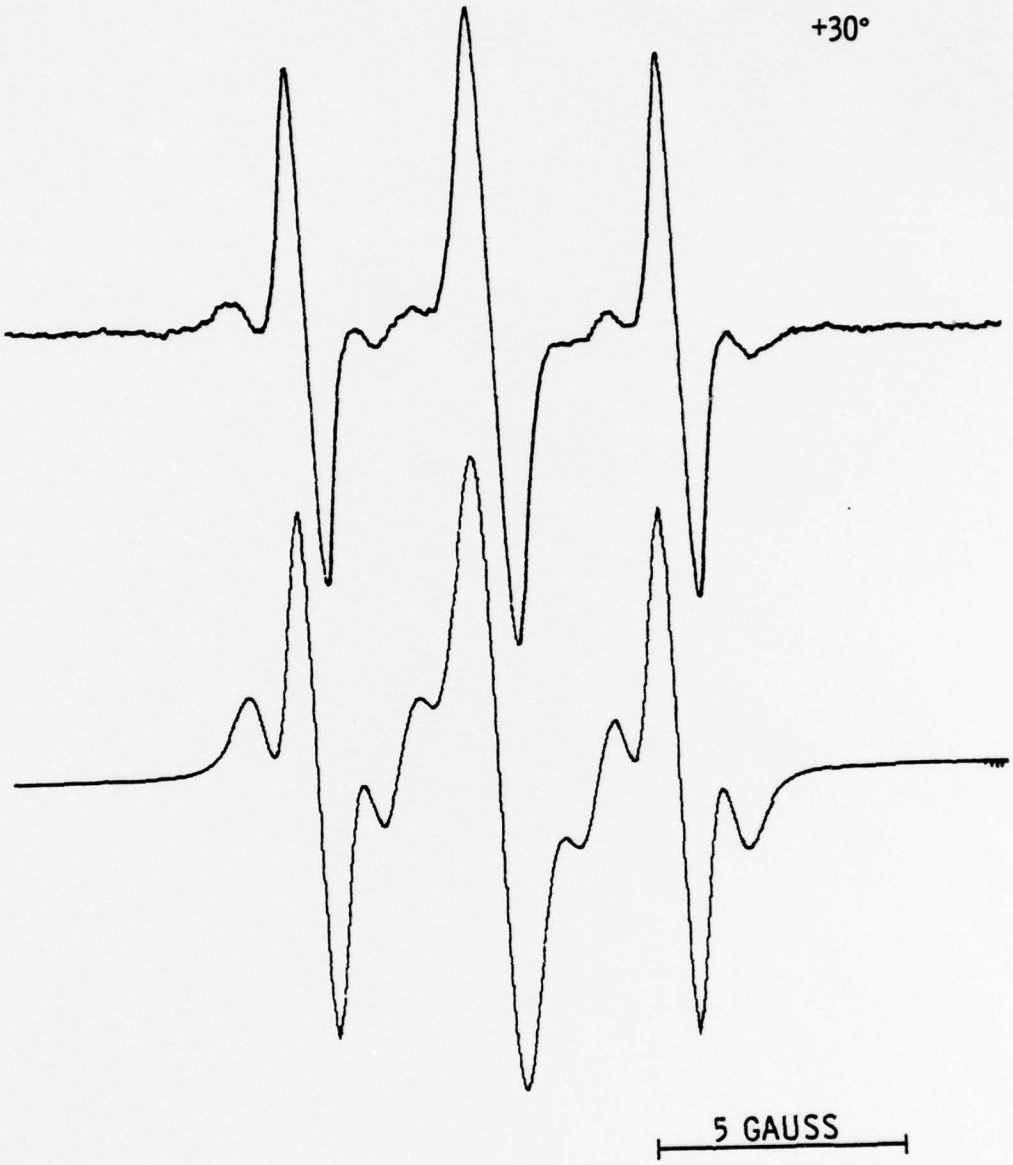

Figure 2

EPR Spectra of $K^{+}TB4N^{-}$ in Dimethoxyethane at 30°C, (upper) and computer simulation of the exchange process of the cation moving to positions on the opposite sides of the aromatic system (see ref. 4 for details).

distribution by the cation. In order to determine the hyperfine splittings in the limit of slow oscillation of the cation about the anion radical, the parameters from K^+, TB4N in tetrahydrofuran, which forms a relatively tight ion pair, had to be used. Rather than observing four lines from two inequivalent protons as expected, 16 lines from four inequivalent protons were observed. These data are summarized in Table III. In order to understand this data in context with the spectra which show splittings from only two protons at the 4- and 5-positions, the two smaller splittings had to be assumed to be of opposite sign. These data were used to compute the spectrum shown in Fig. 2, which shows remarkable agreement with the experimental even reproducing the apparent satellite lines which occur on either side of the three intense lines. The rate of alkali metal motion between opposite sides of the anion radical were determined from these calculations. The interpretations and significance of these experiments are:

The rates of alkali metal motion between opposite sides of the anion were found to either increase or decrease with temperature, depending upon solvent and cation. The apparent activation energy depends on whether the solvation of the cation is highly temperature-dependent. In ethereal solvents, the solvation decreases with temperature, thus increasing the depth of the potential well of the alkali metal cation in the region of the anion. This was the first observation of apparent negative activation energies for this process in ion-paired systems.

In order to explain the hyperfine splittings from the 2- and 7-positions in tight ion pairs, bending must occur at the 1- and 8-positions.

TABLE III

EPR PARAMETERS OF 1,3,6,8-TETRA-TERT-BUTYL NAPHTHALENE ION PAIRS

Cation	Solvent	Hyperfine Splittings	
		4 and 5 Positions	2 and 7 Positions
K^+	Tetrahydrofuran	-3.24 -3.80	±0.84 ∓1.23
Na^+, K^+	Dimethoxyethane	-3.65	<|0.15|

This is sketched in Fig. 3. This is also the first evidence obtained by EPR that bending can occur in ion-paired aromatic hydrocarbons, although X-ray studies show bending in crystals of alkali metal cations with hydrocarbon dianions.(15,16)

The EPR spectra of K^+, 1,3,6,8-tetra-tert-butyl naphthalene$^-$ in tetrahydrofuran showed the presence of two ion pairs which could be unequivocally identified as a tightly bound ion pair and an intermediately bound ion pair by virtue of different proton hyperfine splittings. Because splittings of K^+ ions are small, the nature of ion pairs of aromatic hydrocarbon anions with potassium had never been elucidated with certainty.

The role of the computer in these experiments was in part similar to that described for the studies of the structure of the radical anion. In addition, the computer was also utilized to determine the relative intensities of different lines and their linewidths to estimate the relative concentrations of different ion-paired species.

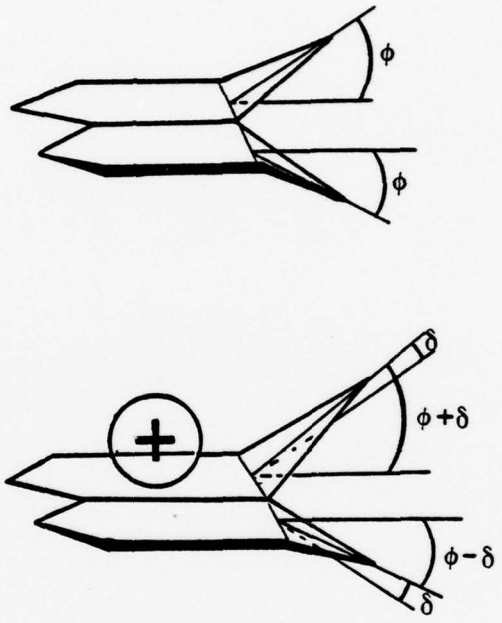

Figure 3

Non planar aromatic system of the 1,8-di-tert-butyl naphalene anions (upper); additional bending through angle δ due to the presence of a cation over the aromatic system.

3.3 Application to Valence-Bond Isomerization

The extreme non-planarity of the 1,8-di-tert-butyl naphthalene anion and the symmetry of the lowest antibonding orbital suggested that the radical ion might isomerize according to the reaction

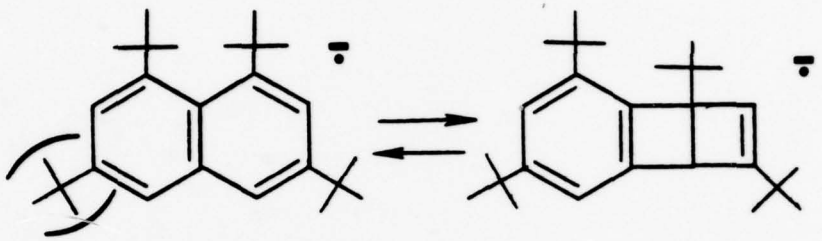

This was found to proceed at low temperatures in a mixture of 60% dimethoxyethane/tetrahydrofuran. The stability of the dewar isomer depended upon the solvent composition and the cation. Apparently, the cation also plays a role in the isomerization process by bending one of the peri-substituted positions further out of the plane allowing the second to become more planar. Kinetics experiments done on 1,3,6,8-tetra-tert-butyl naphthalene reacting to the dewar isomer, shows the second-order dependence, suggesting that the process occurs through the dianion intermediate.[3]

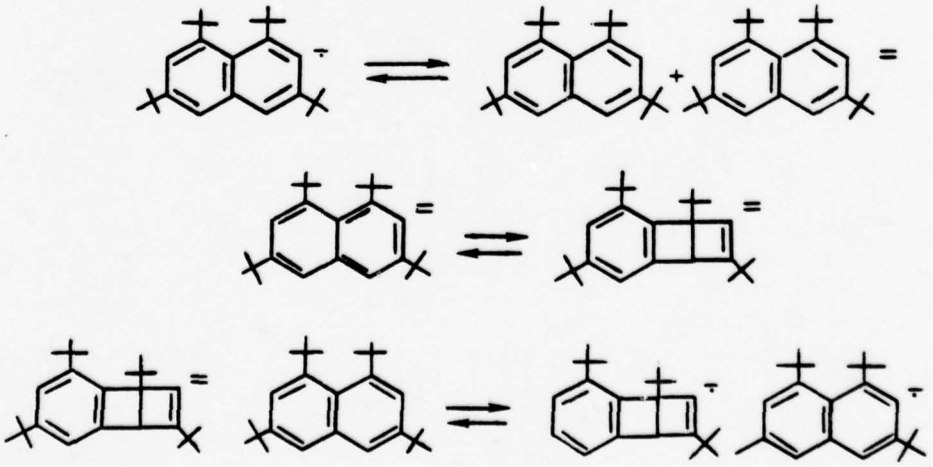

Although several radical ions were observed to isomerize from bicyclic 3-5 rings to 6-membered ring systems, this is the first which has been observed to form a Dewar configuration.

Many of these experiments were carried out in dilute solutions $< 10^{-5}$ M so that again reliable signal averaging was required to observe the spectra. To carry out the kinetics, the sample was equilibrated at a high temperature, and the temperature was reset to the desired value. The thermal equilibration time was about 90-120 s so that only slow reactions could be followed.

3.4 g-Factors and Hyperfine Splittings of Substituted Naphthalene Anions

This research task was taken to evaluate whether the dedicated computer could be used to measure g-factors in a complex spectrum with a greater degree of accuracy than conventional methods, as well as to observe the effects of substitutions of alkyl groups for protons on the electronic structure of radical anions.

The experimental procedure was to record, on a slow sweep, the spectra of the substituted naphthalene anions with a perylene anion reference both on a dual channel strip chart recorder and on two data files recorded simultaneously on the computer. The utility of the computer for analysis of the hyperfine splittings was limited by the fact that in complex spectra overlapping lines could not be separated whereas this is easily done visually. Pattern recognition routines can be used to make this decision, but on spectra

of over 50 lines, this would be a lengthy procedure, and not warranted as far as the limited use planned for the work. The advantage of separating lines on the computer would be to determine a better fit to the spectra than could be done by selecting certain points.

In order to determine the g-factors, the computer was used to determine the absorption maxima (zero-crossing of the derivative) of the center lines of the spectra of the substituted naphthalene anion and the perylene anion reference. The field difference between both samples, δ, was determined by using two perylene anion samples. The g-factor was then calculated by

$$g_s = g_r \left[1 - \frac{(H_s - H_r) - \delta}{h\nu / g_r \mu_B} \right]$$

where g_s and g_r are the g-factors of the sample and reference, and $(H_s - H_r)$ is the field difference between the sample and reference. Values obtained from the computer agreed to within the standard deviation (typically 1.5 ppm = ±0.000003 units).

The hyperfine splittings and g-factors obtained from the measurements were used to establish an optimum value for the inductive effects of the tertiary butyl group to be used with semi-empirical molecular orbital calculations. These values are compared to those of the methyl group determined by Fraenkel et. al. in Table IV. The details of the analysis are presented in Reference 5. It is interesting to note that the parameters for the tertiary-butyl group are about 1/2 of those for the methyl group. We do not understand

TABLE IV

INDUCTIVE PARAMETERS FOR METHYL- AND TERT-BUTYL SUBSTITUTION

	Methyl	Tert-Butyl
Hyperfine Splittings	-0.14 ± 0.04[1]	-0.07 ± 0.02
g-Factors	-0.50 ± 0.10	-0.30 ± 0.08
Alkyl Splittings	-0.31 ± 0.01[1]	Not observed

[1] Ref. 18.

why those values determined from the g-factor are different than for the α-proton hfs, although this trend is observed for both the methyl and tertiary-butyl substituents. The values determined from the g-factor are close to those determined from the electronic spectra.

4.0 STUDIES ON THE FORMATION OF NF_4^+ SALTS

The mechanism of the formation of NF_4^+ salts[20] such as $NF_4^+SbF_6^-$ and $NF_4^+BF_4^-$ by the UV photolysis of F_2, NF_3 and the corresponding Lewis acid, XF_n,

$$F_2 + NF_3 + XF_n \xrightarrow[\text{heat}]{h\nu \text{ or}} NF_4^+ XF_{n+1}^-$$

had not been established. While it has been accepted that the initial step of the reaction is

$$F_2 \xrightarrow{h\nu} 2F^{\bullet} \qquad (1)$$

several mechanisms could be invoked to describe the formation of the NF_4^+ salts.

Both constant and pulse UV-radiation was used to study the reaction. A broad signal was observed during constant irradiation which by signal averaging and generating the 2nd derivative was found to be the $NF_3^{+\bullet}$ radical by analogy to the spectrum observed by Symons et. al.[21] Pulse radiation showed a rapid rise of the EPR signal, but only a very slow decay at 77°K. From these observations, the following mechanism was proposed for the synthesis of NF_4^+ salts:[10]

$$F^{\bullet} + XF_n \rightarrow XF_{n+1}^{\bullet} \qquad (2)$$

$$XF_n^{\bullet} + NF_3 \rightarrow NF_3^{+\bullet} XF_{n+1}^- \qquad (3)$$

$$NF_3^{+\bullet} XF_{n+1}^- + F^{\bullet} \rightarrow NF_4^+ XF_{n+1}^- \qquad (4)$$

The fact that $NF_3^{+\bullet}$ is stable, suggests that reaction of $NF_3^{+\bullet}$ with F_2,

$$NF_3XF_{n+1}^- + F_2 \rightarrow NF_4^+XF_{n+1}^- + F^\cdot \qquad (5)$$

is not significant. Thus, the following conclusions were reached: 1) $NF_3^{+\cdot}$ is an important intermediate in the synthesis, 2) reactions 1, 2, and 4 are consistent with the need for UV activation and 3) the chain propagation step, reaction 5, does not play an important role. The xF_{n+1} radicals, while probably are produced, is not detected due to its expected short relaxation time.

A consequence of this study is that by using spectra presented in the literature[21] for $NF_3^{+\cdot}$, we found that the analysis was incorrect. As a result we remeasured the spectrum.[22] Most important, we found that the $NF_3^{+\cdot}$ radical was stable at room temperature for several weeks, and that the nitrogen and fluorine hfs were incorrectly assigned. Thus we concluded that $NF_3^{+\cdot}$ is more planar than $CF_3^\cdot$ rather than less as previously assumed.

5.0 STUDIES ON 1,3,6,8-TETRAMETHOXYTHIANTHRENE

Photogenerated triplet states of thianthrene and 2,3,7,8-tetramethoxythianthrene were studied by EPR.[6] Values of D^* were obtained

$$D^* = (D^2 + 3E^2)^{1/2}$$

where D is given by $3g^2\beta^2/4\cdot(r^2 - 3z^2/r^5)$, E is $3g^2\beta^3/4(x^2 - y^2/r^5)$, x, y, and z refer to the molecular coordinates of the electron and r is the interelectron distance. The value of D^*, therefore, reflects the interelectron separation. Values of D^* for the lowest energy triplet states of thianthrene and tetramethoxythianthrene were determined. Lifetimes of these states were also determined using flash photolytic techniques. A sample of the dication of 2,3,7,8-tetramethoxythianthrene was also found to be in a ground state triplet configuration, with an energy of about 140 cm^{-1} below that of the lowest energy singlet state. Typically, only molecules which exhibit greater than three-fold symmetry or those which have two non-interacting segments such as nitroxide groups coupled by an alkyl linkage will have a triplet ground state. Thus the tetramethoxythianthrene cation is indeed an anomaly.

The role of the computer in this study was to average weak spectra as before; but it was also used to determine the decay rates of the photogenerated triplet states. The amplitude of the $\Delta m = 2$ transition was used as a measure of concentration. Magnetic field stability and lamp recharing were monitored by the computer. At liquid nitrogen temperature the triplet state was found to decay rate constant of 20 s^{-1}.

The spectra of the tetramethoxythianthrene cation was also studied using the computer controlled system and the g-factor and hyperfine splittings were measured. Signal averaging permitted accurate determination of the ^{33}S hfs.

6.0 DEVELOPMENT OF EPR-ANALYTICAL TECHNIQUES

During the course of this work we have greatly improved the analytical precision of EPR. In ascertaining the nature of these problems we have also prepared a review of analytical EPR.[7]

One of the major advantages of utilizing EPR as an analytical tool for paramagnetic species, is that it can be calibrated by virtually any other paramagnetic material, provided the sample cell and geometry is kept the same. Researchers have generally assumed that EPR is only capable of about ±10% precision in this mode of operation.[23,24] Reasons for the poor precision that has been reported have been ascribed to uncertainty of the zero point in the derivative curve, baseline drift, and truncation of the tailing portions of the spectra. Utilizing the computer, we have found methods of overcoming these difficulties.

Baseline drift is significant at high amplifications of the EPR signal, probably because magnetostriction slightly alters the cavity geometry. (Not because of eddy currents or interaction of the rf field with the static field, as commonly assumed.) Consequently it is reproducible, and reliably subtracted from the spectrum of the unknown by utilizing the computer.

Using the property that the integral of the derivative curve is zero, the baseline of the spectrum can also be defined by taking the average of all of the data points. If this is done sufficiently far into the wings of the line, then broadening due to field inhomogeneities become insignificant,

whereas if this process is done with only a few data points, the baseline will be erroneous. This is quite critical, because an error in the baseline determination enters the final result as a square term as well as a linear term. We feel that this has also been a major source of error in previous analyses, since it has been reported[24] that when each half of the first derivative curve is separately double-integrated the results are not equal. This probably results from an inhomogeneous magnetic field which causes a small amount of line distortion.

Finally, most EPR lines are very nearly Lorentzian in character. Since the behavior of these lines is well defined, the computer is also used to calculate the correction to the double integral from an analysis of the lineshape.[9] Representative double integrals for O_2 at different pressures are given in Table V. The correction factor for a Lorentzian line is given by the equation

$$f = \left\{ \frac{\pi}{2} + \frac{(H_s - H_o)/\Gamma}{\left[1 + \frac{(H_s - H_o)^2}{\Gamma^2}\right]} - \tan^{-1}\left(\frac{H_s - H_o}{\Gamma}\right) \right\}^{-1}$$

for a double integration which is symmetric about the resonance center of the line, where H_s is the starting field, H_o is the resonance field, and Γ is the half-width at half height. The factor f is calculated by the computer. Note that utilizing the correction factor, the precision of the corrected intergrals in Table V are improved. This improvement would be more evident if the value of scan/ΔH_{pp} had a larger range. Note that the uncorrected integral

TABLE V

DOUBLE INTEGRAL VALUES OF O_2 LINES

Pressure* P(Torr)	Gain G	Modulation H_m(Oe)**	Scan (ΔH_{pp})	$\frac{I}{P\ G\ H_m}$	Correct. Factor	I Corrected
0.096	100	0.125	21.3	4.518	1.115	5.038
0.096	80	0.160	21.3	4.453	1.115	4.965
0.096	125	0.100	21.3	4.414	1.115	4.922
0.175	63	0.125	18.3	4.317	1.136	4.904
0.175	50	0.160	18.3	4.400	1.136	4.998
0.175	80	0.100	18.3	4.309	1.136	4.895
0.312	50	0.125	17.1	4.403	1.147	5.050
0.312	40	0.160	17.1	4.391	1.147	5.036
0.312	63	0.100	17.1	4.372	1.147	5.015
0.414	40	0.125	16.7	4.323	1.151	4.976
0.414	50	0.100	16.7	4.312	1.151	4.963
0.414	32	0.160	16.7	4.281	1.151	4.927
0.518	50	0.125	15.7	4.309	1.162	5.007
0.518	40	0.160	15.7	4.309	1.162	5.007
0.518	32	0.200	15.7	4.320	1.162	5.020
0.697	63	0.125	15.0	4.395	1.170	5.142
0.697	50	0.160	15.0	4.322	1.170	5.056
0.857	63	0.125	14.5	4.248	1.177	5.000
0.857	50	0.160	14.5	4.233	1.177	4.982
0.857	40	0.200	14.5	4.217	1.177	4.963
0.999	63	0.125	13.6	4.230	1.191	5.038
0.999	50	0.160	13.6	4.130	1.191	4.919
0.999	32	0.250	13.6	4.202	1.191	5.004
		Mean Value		4.324		4.998
		Standard Deviation		0.089		0.065
		Relative Error		2.1%		1.3%

*Pressure is accurate to ± 9.5%.
**H_m is defined by $H(t) = H_m \cos(wt)$.

decreases systematically as the relative scan width decreases. Using the correction factor, there is no such systematic error. Also important is the fact that the magnitude of the corrected double integral is 15% greater than the uncorrected value. This factor is not important for a single species, but is critical when different standards are to be used. The number of data points which are utilized also appears to affect the results. For an ideal lineshape, e.g., $Cr(NO_3)_3$ in H_2O, which is Lorentzian, we have found that the best magnetic field range over which to integrate the signal is about 6-10 times the peak-to-peak width. The reason for this is that the noise will add as the square root of the number of data points used in the analysis, while the signal adds as the reciprocal of the square of deviation from resonance in the wings of the line. In this way we have been able to detect 5×10^{-6} M Cr^{3+} with an accuracy of ±2%, for example, based on using a $MnSO_4$ solution to calibrate the spectrometer.

By making careful use of the integration techniques we have developed, we have shown[8] that EPR can yield non linear analytical results when large samples are used in the cavity. This is because the EPR signal s is proportional to the microwave power reflected from a cavity and depends on the change of its Q-factor from the off resonance Q-factor, Q_o,

$$S \propto \frac{Q - Q_o}{Q_o} = \frac{4\pi\eta Q_o \chi''}{1 + 4\pi\eta Q_o \chi''}$$

where η is the filling factor of the cavity and χ'' is the imaginary component of the microwave susceptibility proportional to the number of paramagnetic

sites and the spin.[2] From theoretical calculations, as well as empirical measurements, it was concluded that a 1% error can be obtained in conventional measurements with samples as large as: 0.05 M $MnSO_4$ solution, 0.25 mg of DPPH, or 1.0 mg $MnSo_4 \cdot H_2O$. The error increases rapidly as the sample size increases. It was also found that the parameter least sensitive to analytical error was the square of the linewidth multiplied by the peak-to-peak amplitude.

7.0 STUDIES ON OTHER CHEMICAL SYSTEMS

7.1 Maleate-Fumarate Esters

Interest in the isomerization of maleate-fumarate esters

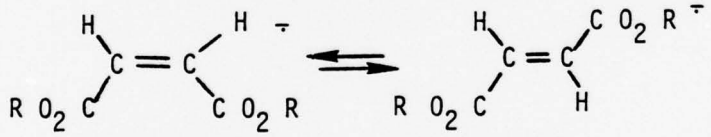

(Maleate) (fumarate)

came from the fact that identical spectra were reported for the anion radicals of dialkylmaleates and fumarates,[25,26] and the spectra corresponded to mixtures of the equilibrium concentrations of the isomers. More recently, this was interpreted as four isomers of the fumarate anion, which may have the structures shown in Fig. 2a.[27] In order to distinguish between these explanations, we prepared the cyclic compounds,[28]

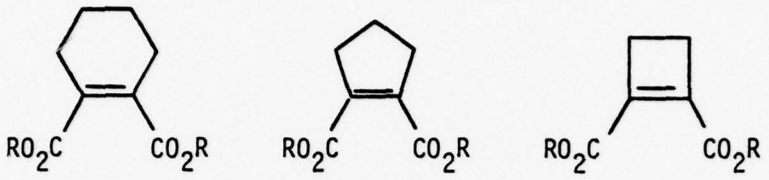

which are analogous to the maleate isomers, but they are locked in the cis-configuration.

Solutions in dimethylformamide using tetrabutylammonium iodide supporting electrolyte were studied by electrochemical and electrochemical-EPR methods. Apparently, the cyclic compounds deposit as an insulating film on the platinum electrodes. No identifyable spectra were obtained. Studies of the maleate isomers yielded spectra similar to those of the fumarate, but weaker. The intensity of the portion of the signal could well be that there is several percent fumarate in the maleate, as detected by nuclear magnetic resonance of the diethyl and dimethyl maleates.

These results are consistent with the conclusions of Bard, et.al,[19] that cis-olefinic anion radicals dimerize very rapidly. Pulse EPR electrochemical studies revealed equal decay rates for the weaker lines and the stronger lines in the dimethylfumarate anion spectra. We conclude therefore, that the observed EPR spectra are indeed due to fumarate ions in agreement with Nelsen and Gillespie, but our interpretation differs in one respect. While they identify four species, two of which give rise to very weak lines, we identify three species, two of which are due to the more intense lines, and

the third is due to the weaker lines. In our interpretation, the species which gives rise to the weakest spectrum does not have equivalent olefinic protons. This interpretation is consistent with free rotation about the C-OR bond at high temperatures. Thus, the isomers α and γ will have pairs of equivalent olefinic protons, while β has two inequivalent olefinic protons. Our analysis of this spectrum is shown in Table VI and is compared to that of Nelson and Gillespie.[17] Proof of this analysis would have required extensive time and modification of our EPR-electrochemical cell. Since this aspect of olefinic systems is of limited interest, it was not continued.

TABLE VI

ANALYSIS OF THE DIMETHYLFUMARATE ANION SPECTRUM

Species	Proton*	hfs	hfs, Nelson[17]
1	Methyl	(6) 1.38	(6) 1.39
	Olefinic	(2) 6.61	(2) 6.62
2	Methyl	(6) 1.38	(6) 1.39
	Olefinic	(2) 6.82	(2) 6.83
3	Methyl	(6) 1.36	(6) 1.35
	Olefinic	(1,1) 6.83, 6.63	(2) 6.73
4	Methyl		(6) 1.35
	Olefinic		(2) 6.73

*Numbers of equivalent protons in parenthesis.

7.2 Gas Phase Reactions of Fluorine Atoms

It would be of interest to be able to study the reactions of atomic fluorine with hydrogen donors or with acceptors (e.g., olefins, O_2) in the gas phase using EPR, since F gives a strong signal, eliminating the need for vacuum UV techniques or indirect measurement. Nevertheless, using UV pulses, weak signals were obtained. Using steady state photolysis, a very slow buildup was observed. When the light was turned off, the signal decayed rapidly, and turning the lamp on again resulted in only a slow increase in the signal. We have no explanation for this behavior, other than the possibility that there is some surface contamination. If this is correct, only a very large volume to surface ratio would be practical for transient studies of F, which is not practical with the fixed-geometry EPR apparatus. Although different surfaces were studied (quartz, HF-washed quartz, halocarbon wax coating, and phosphate coating), the same results were obtained.

Separate studies, using NO to react both F and F_2,

$$F + NO \xrightarrow{He} FNO$$

$$F_2 + NO \longrightarrow FNO + F$$

demonstrated that the loss of signal was due entirely to F-atom recombination and not to chemical reaction of F with impurities. We do not understand the origin of this enhanced recombination.

8.0 COMPUTATIONAL TECHNIQUES

8.1 Smoothing Algorithm

Signal averaging while very useful in improving signal-to-noise ratio, are subject to instrumental instabilities, long time durations, and large sample quantity requirements. It is therefore advantageous to utilize computational methods for improving signal to noise. Secondly, it is sometimes desirable to generate the second derivative of a spectrum for resolving shoulders, or diminishing the extent of a broad signal. This increases the noise.

Several different Fourier smoothing techniques have been used. However, these often affect the lineshape. As a result, we have used a median technique[30,31] with remarkable success. An outline of this method is given in Eqs (1) to (8) were x_i is the initial data file and x_i' is the transformed data,

$$a_i = \text{med}\left\{x_{1-2},\ x_{i-1},\ x_i,\ x_{i+1},\ x_{i+2}\right\} \tag{1}$$

$$b_i = \text{med}\left\{a_{i-1},\ a_i,\ a_{i+1}\right\} \tag{2}$$

$$c_i = \frac{1}{4}\left(b_{i-1} + 2b_i + b_{i+1}\right) \tag{3}$$

$$r_i = x_i - c_i \tag{4}$$

$$d_i = \text{med}\left\{r_{i-2},\ r_{i-1},\ r_i,\ r_{i+1},\ r_{i+2}\right\} \tag{5}$$

$$e_i = \text{med}\left\{d_{i-1},\ d_i,\ d_{i+1}\right\} \tag{6}$$

$$f_i = \frac{1}{4}\left(e_{i-1} + 2e_i + e_{i+1}\right) \tag{7}$$

$$x'_i = c_i + f_i \tag{8}$$

This smoothing process can be used for any number of adjacent points. We have primarily used the method given above as well as an abbreviated series in which medians of three adjacent points are used if relatively narrow lines are detected. Although this was originally intended for use after taking derivatives, we have found a significant improvement in signal-to-noise, and thus saving considerable time in data collection when applying this to raw data. We have also found that using the median processing does not significantly affect he value of the double integral of the EPR signal. Thus we have been able to measure 10^{-7} M Mn^{2+} concentrations to ±2%.

Initially, when generating the derivative, the difference between adjacent data points was used. However, a report[32] tabulated coefficients of the Lagrangian interpolation equations in which 3 to 7 adjacent points could be used in the derivative. Specific sets of coefficients were incorporated in an off-line program and yielded much smoother derivative curves than did the use of adjacent lines. To further smooth data, the above median smoothing process was utilized.

8.2 Integration Using Fast Fourier Transform

At this point, the method of using the fast Fourier transform to doubly integrate the derivative spectrum can offer several advantages. First of all, it offers the possibility of subtracting any baseline offset implicitly in the program. Secondly, it treats frequency space rather than time space, so that errors may not compound as readily. Using the Fourier transform methods, we have succeeded in generating absorption curves from the first-derivative spectra, but an artifact in the mathematical processing causes the double integral to appear rotated so that the initial and final values are zero. As this procedure would be useful in many areas in which we are currently working, we hope to complete this work and submit it for publication in the near future.

9.0 REFERENCES

1. I. B. Goldberg, H. R. Crowe, and R. S. Carpenter, II, J. Magn. Resonance 18, 84 (1975).

2. I. B. Goldberg, H. R. Crowe, and R. W. Franck, J. Phys. Chem., 79, 1974 (1975).

3. I. B. Goldberg, H. R. Crowe, and R. W. Franck, J. Am. Chem. Soc., 98, 7641 (1976).

4. I. B. Goldberg and H. R. Crowe, J. Phys. Chem., 80, 2603 (1976).

5. I. B. Goldberg and B. M. Peake, J. Phys. Chem., 81, 571 (1977).

6. I. B. Goldberg, H. R. Crowe, G. S. Wilson, and R. E. Glass, J. Phys. Chem., 80, 988 (1976).

7. I. B. Goldberg and A. J. Bard, "Analytical Applications of Electron Paramagnetic Resonance" in Treatise on Analytical Chemistry, 2nd ed. I. M. Kolthoff, D. J. Elving and M. Bursey, eds. in press.

8. I. B. Goldberg and H. R. Crowe, Anal. Chem., 49, 1353 (1977).

9. I. B. Goldberg, J. Magn. Reson., 32, 233 (1978).

10. K. O. Christe and I. B. Goldberg, Inorg. Chem., 17, 759 (1978).

11. J. B. Phillips, M. F. Burke, and G. S. Wilson, Computers in Chem., in press.

12. R. Hirasawa, T. Mukaibo, H. Hasegawa, Y. Kanda, and T. Maruyama, Rev. Sci. Instrum., 39, 935 (1968).

13. E. S. P. Hsi, L. Fabes, and J. R. Bolton, Rev. Sci, Instrum., 44, 197 (1973).

14. J. Handel, J. G. White, R. W. Franck, Y. H. Yuh, and N. L. Allinger, J. Am. Chem. Soc., 99, 3345 (1977).

15. P. D. Sullivan and J. R. Bolton, Adv. Magn. Reson., 4, 39 (1970).

16. J. J. Brooks, W. Rhine, and G. D. Stucky, J. Am. Chem. Soc., 94, 7346 (1972).

17. W. E. Rhine, J. Carvis, and G. Stucky, J. Am. Chem. Soc. 97, 1079 (1975).

18. R. E. Moss, N. A. A. Ashford, R. G. Lawler, and G. K. Fraenkel, J. Chem. Phys., 51, 1765 (1969).

19. A. Streitweiser, Jr., "Molecular Orbital Theory for Organic Chemists," John Wiley, N. Y. 1961, Chapter 5.

20. K. O. Christe, C. J. Schack, and R. D. Wilson, Inorg. Chem. 15, 1275 (1976).

21. S. P. Mishra, M. C. R. Symons, K. O. Christe, R. D. Wilson, and R. I. Wagner, Inorg. Chem., 14, 1103 (1975).

22. I. B. Goldberg, H. R. Crowe, and K. O. Christe, Inorg. Chem., 17, 3789 (1978).

23. M. L. Randolph, "Quantitative Considerations in Electron Spin Resonance Studies of Biological Materials" in Biological Applications of Electron Spin Resonances, H. M. Swartz, J. R. Bolton, and D. C. Borg, Eds, Wiley, New York 1972.

24. A. A. Westenberg, Progr. React. Kinetics, 7, 23 (1973).

25. S. F. Nelsen, Tetrahedron Lett, 3795 (1976).

26. I. H. Elson, T. J. Kemp, D. Greatorex and H. D. B. Jenkins, J. Chem. Soc., Farady Trans. II, 69, 1402 (1973).

27. S. F. Nelson and P. J. Gillespie, J. Org. Chem. 40, 2391 (1976).

28. R. N. McDonald and R. R. Reitz, J. Org. Chem. 37, 2418 (1972).

29. A. J. Bard, V. J. Puglisi, J. V. Kenkel and A. Lomax, Faraday Disc. 56, 353 (1973).

30. K. Enslein, private communication.

31. L. R. Rabiner, M. R. Sambur, and C. E. Schmidt, IEEE Trans. ASSP-23, 552 (1975).

32. H. E. Salzer, "Table of Coefficients for Obtaining the First Derivative without Differences," NBS Applied Math. Ser. 2, April 1948.

10.0 PERSONNEL

I. B. Goldberg - Principal Investigator

H. R. Crowe - Computer Programming, Conducting EPR Experiments

R. S. Carpenter - Computer Programming

J. J. Ratto - Synthesis of cyclic di-carboxy esters

11.0 TECHNICAL REPORTS

1. I. B. Goldberg, H. R. Crowe, and R. S. Carpenter, III, "Computer Control of Electron Spin Resonance Spectroscopy," J. Magn. Resonance 18, 84 (1975).

2. I. G. Goldberg, H. R. Crowe, and R. W. Franck, "Peri-Interactions in the 1, 3, 6, 8-Tetra tertpbutyl- and 1, 3, 8-Tri-tert-butylnaphthalene Anions: An EPR Study," J. Phys. Chem. 79, 1974 (1975).

3. I. B. Goldberg, H. R. Crowe, G. S. Wilson, and R. E. Glass, "The 2,3,7,8-tetramethoxythianthrene Dication, An Unusual Ground State Triplet, the Photogenerated Triplet, and the Cation Radical," J. Phys. Chem. 80, 988 (1976).

4. I. B. Goldberg and H. R. Crowe, "EPR Study of the Association of 1,8-Di-tert-butylnaphthalene Anions with Sodium and Potassium Cations," J. Phys. Chem., 80, 2603 (1976).

5. I. B. Goldberg and B. M. Peake, "EPR Spectra of tert-Butyl Substituted Naphthalene Anions," J. Phys., Chem. 81, 571 (1977).

6. I. B. Goldberg, H. R. Crowe, and R. W. Franck, "An Unusual Reversible Valance Bond Isomerization: Hemi-Dewar Naphthalene," J. Am. Chem. Soc., 98, 7641 (1976).

7. I. B. Goldberg and A. J. Bard, "Analytical Applications of Electron Paramegnetic Resonance," Treatise on Analytical Chemistry, 2nd. Ed., I. M. Kolthoff, P. J. Elving, and M. Bursey, eds, in press.

8. I. B. Goldberg and H. R. Crowe, "Effect of Cavity Loading on Analytical Electron Spin Resonance," Anal. Chem., 49, 1353 (1977).

9. K. O. Christe and I. B. Goldberg, "EPR Evidence of the Formation of the NF_3^+ Radical Cation as an Intermediate in the Synthesis of NF_4^+ Salts by Low Temperture UV-Photolysis," Inorg. Chem., 17, 759 (1978).

10. I. B. Goldberg, "Improving the Analytical Accuracy of Electron Paramagnetic Resonance Spectroscopy" J. Magn. Reson., 32, 233 (1978).

APPENDIX 1

COMPUTER CONTROL OF ELECTRON SPIN RESONANCE SPECTROMETRY

JOURNAL OF MAGNETIC RESONANCE 18, 84–96 (1975)

Computer Control of Electron Spin Resonance Spectroscopy

IRA B. GOLDBERG, HARRY R. CROWE, AND RICHARD S. CARPENTER, II

Science Center, Rockwell International, Thousand Oaks, California 91360

Received August 16, 1974

A laboratory computer interface with an electron spin resonance (ESR) spectrometer is reported, which permits operator control of the magnetic field through the computer. Two programs are described. In the first, the field is stepped and checked for stability at preset increments before data from a signal channel and a reference channel are collected. Any number of increments can be accumulated, and the signal channel can also be recorded as a function of time. The second program uses a continuous sweep to collect data. Sweep rates up to 10 kG/min have been used with no auxiliary coils. The data acquisition program is started by a signal from the reference channel, and the reference absorptions are counted on the return sweep to insure reproducible starting fields. Signals from the reference or from the sample channels can be recorded during a sweep. Both programs are sufficiently open so that other peripheral functions can be executed.

INTRODUCTION

For more than 10 years, electron spin resonance (ESR) has been used to investigate transient radicals generated by photochemical, electrochemical, and gamma or electron irradiation processes. In more recent years techniques have been developed that allow kinetic parameters as well as structure to be determined from ESR measurements using flash photolysis (*1–4*), pulse electrolysis (*5–7*) and pulse radiolysis (*8,9*). In general, these measurements consist of a synchronized pulse perturbation with a signal averaging device to record the signal time behavior. To obtain information for kinetic analysis the field is held constant and the signal-time behavior is averaged. Spectra are obtained by the additional synchronization of a field sweep by auxiliary coils (*10–12*) with the signal-averaging device and the pulse excitation so that all three processes are initiated simultaneously and the signal is again recorded linearly with time. By assuming that the field varies linearly with time, the ESR signal as a function of field is obtained after the averaging process is completed. The auxiliary coils are placed around the ESR cavity and a voltage or current profile is used to sweep the field. These coils are limited to sweep fields of ±25 to ±100 G from the static magnetic field of the electromagnet. Several problems inherent in this technique (*13*) are 1) the fields are often nonlinear with time; 2) the auxiliary field may disrupt the static magnetic field of the electromagnet; 3) $i \cdot R$ heating for low-resistance coils limits the maximum field, or inductance of coils with many turns limits the degree of linearity with time; and 4) the field homogeneity decreases as the applied field increases.

Although these techniques have been extremely valuable, they do not permit the experimenter to store sufficient data to recreate the ESR spectrum conveniently as a function of time. This would be valuable for systems in which there are several intermediates. For example, a typical signal-averaging device, a computer of average

transients (CAT), has a maximum of 4,096 storage locations. Atkins *et al.* (*2*), have been partially successful in this type of experiment using a CAT, but the technique is not convenient. In addition, the CAT does not in general allow a sample signal and a reference signal to be recorded simultaneously.

A second application where the CAT has been employed is in studies using flow systems. When systems are studied in which rapid reactions occur, the signal-to-noise ratio is usually very low. To enhance the signal, either a long filtering-time constant is required or the field is swept repeatedly and the signals are again stored on the CAT. When a long filtering-time constant is used, it is necessary to insure that the lock-in amplifier is stable and that the magnetic field does not drift. In the latter case, when the field is swept, it is necessary to insure that the CAT starts accumulating at the same field and that the sweep rate is reproducible.

Interactive computer control of the ESR can facilitate each of the experiments described above. Although both small (*14–16*) and large (*17–22*) computers have been used for data acquisition or signal averaging and data analysis, they have not been programmed to interact with the ESR spectrometer in such a way as to optimize conditions for maximum resolution and to facilitate study of transient intermediates.

In this paper we report preliminary results of using a mini-computer to control the magnetic field and accumulate data. It is programmed to acquire data only when certain operating conditions are met. In addition, it permits the operator to view the experimental results following each experiment and therefore allows decisions concerning succeeding experiments to be made. Two methods of acquiring data are described here. One method uses a swept field. The signal is recorded as a function of time and the data acquisition is initiated at precisely the same field. The other method uses a sequentially stepped field in which the step size can be made to depend upon the previous signal, and data are recorded after the field has stabilized. Succeeding work will deal with specific applications of computer control to problems in ESR.

EXPERIMENTAL

The ESR spectrometer system consists of the console of a V-4502 spectrometer which contains the AFC, klystron power supply, klystron mode sweep and oscilloscope circuitry, and a 100 kHz field modulation apparatus. The microwave bridge is a reflection homodyne using a TE104 dual cavity, three-port circulator, Schottky diode detector, and a microwave bucking arm (*23*). A second channel capable of modulation amplitudes from 0.005 to 100 G-peak-to-peak between 0.1 and 50 kHz was constructed as described in Ref. (*24*). The magnet used in this system is a Magnion 15 in. magnet (O. S. Walker) with an FCC-4 controller. This particular controller is easily adaptable to computer interfacing because it provides an input that permits field steps of ± 5, 50, 500 or 5,000 G/V relative to a value preset on the controller by the operator. In this way the magnitude of the field can be controlled to the desired accuracy by a digital-to-analog converter (DAC). A full-wave rectified 30-cycle signal output, which is proportional to the value of the field deviation from the preset value, is also provided. This output permits both the control and measurement of field. Although we have not found it necessary, a very simple modification can be made to the controller to enable the sweep rate of the magnetic field to be controlled by the computer. The magnetic field drift, measured with a proton resonance probe was within 2 ppm/hr after 1 hr of

warm-up time. Sweep rates up to 10,000 G/min are also provided. Measurements at rates up to 100 G/min were found by first order least squares to be linear to better than 0.02% and reproducible to 0.02%. Modifications to other magnet systems to permit external voltages to control magnetic fields have been reported (*25*, *26*).

The laboratory computer is a commercial "Data Acquisition System" (Science Center, Rockwell International) and consists of Digital Equipment, PDP 8/m, with 16 K 12-bit words of core memory, extended arithmetic facility real-time clock, and an RK05 disk with a capacity of 1.6 million words. Auxiliary equipment includes a

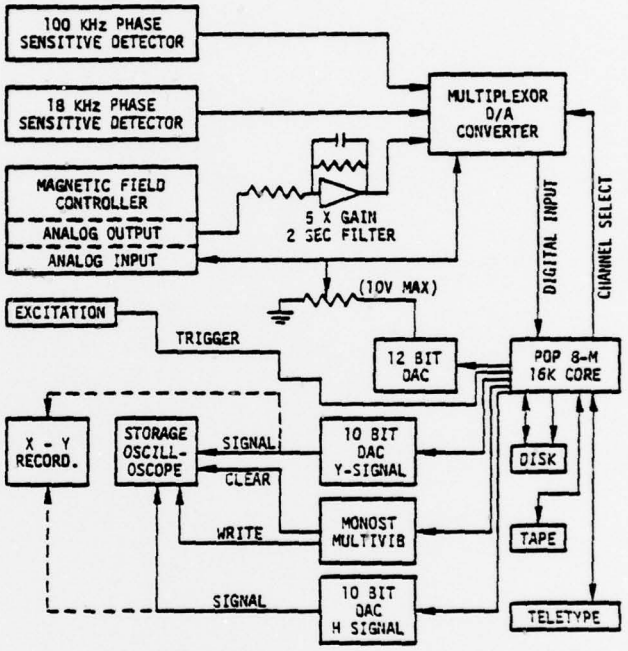

FIG. 1. Interface of the PDP 8/m computer with an ESR spectrometer.

9-track tape (Pertec Corp.), 48-channel multiplexer-12-bit analog-to-digital converter which has a selection and conversion time of 40 μsec (Xincom Corp.), several 10-bit and one 12-bit DAC outputs, teletype control and a Tektronix 611-storage oscilloscope. A diagram of the computer-ESR interface is shown in Fig. 1. The tape is used for permanent storage and most experimental work is carried out using the disk and core memory. DAC's are used for field control and display purposes.

PERFORMANCE OF THE SYSTEM

The approaches to data acquisition from the ESR spectrometer that are described here are the stepped field method, in which the field is incremented and allowed to stabilize before recording data, and the swept field method in which the magnet is allowed to sweep and reverse automatically. Data acquisition is triggered by a reference

signal. Both of these methods permit an excitation such as a flash lamp, electrochemical apparatus (constant current or constant potential), or laser to be triggered at any time during the experiment. They also permit both a sample and a reference signal to be recorded. The discussion here is limited to programs that are sufficiently versatile to permit extensions to specific problems, but, in this work, the programs are used to acquire data from stable paramagnetic samples.

Stepped Field Program

In the stepped field program, the magnetic field is sequentially stepped at preset increments to cover a given range of magnetic field. The 30-Hz full-wave rectified signal from the field controller, which is proportional to the difference between the actual magnetic field and the magnetic field set by the operator on the control panel, is amplified by five and filtered through a 2 sec RC filter (see Fig. 1). This signal along with the signals from the 100-kHz and 18-kHz detectors are connected to three channels of the multiplexor-analog-to-digital converter. The output of the DAC used to control the field is led to a ten-turn potentiometer to divide the signals. This improves the resolution of field control and is necessary if a 10-bit DAC is used; but even for a 12-bit DAC, with a resolution one part in 4,095, the smaller output permits finer control of the magnetic field. This output voltage is led to both the multiplexor and to the magnetic field controller.

Most of this program is written in Fortran II, and the mnemonic assembly language "SABR." Sections of the program are "chained together" in order to minimize the amount of core memory required for the program. An abbreviated flow chart is shown in Fig. 2. The computer program is written with data that were previously measured to a high degree of accuracy, such as the number of volts input and output, to obtain a "full scale" field. The full scale field is arbitrary and is either 10, 100, 1,000 or 10,000 G, as set by a manufacturer, and in this case relates to a four-decade attentuator. A field of five times the full scale value can be obtained with a linear relationship between output field and input voltage. The operator tunes the ESR, and starts the program. The program sets the output DAC to 7777 octal and waits for a keyboard input. This allows the output potentiometer to be manually set so that the magnetic field will cover a range equal to or slightly greater than the desired field span (see Fig. 1). When ready, the operator continues the program through the keyboard. First, the output of the potentiometer is read, and the DAC is cleared. The following data are entered by the operator via the teletype: initial field deviation, maximum field deviation, field increment, number of times to read the signal, the "full scale" field described above, and a 1 or a 0 which determines whether or not the reference channel signal is read. The program now calculates the number of units necessary to increment the DAC to obtain the desired size of field step and also calculates the voltage outputs from the field controller which correspond to the initial and final field values.

The value of the increment loaded into the DAC, which would cause the field to change by one increment, and the actual value, which would be loaded into the DAC in order to obtain the exact desired field are calculated in floating point format. Since the DAC has a resolution of one, part in 4,095, the number loaded into the DAC is rounded off, but the floating point value is retained and used to calculate the next value to be loaded. The purpose of doing this is to eliminate a roundoff error in the field

increment, which could amount to as much as 50% if a two-unit per increment change is required, and to eliminate a cumulative error caused by truncating the number to be applied to the DAC. The result of this method is that the field step sizes will not be uniform. This is unimportant because the actual field value is determined from the magnet output.

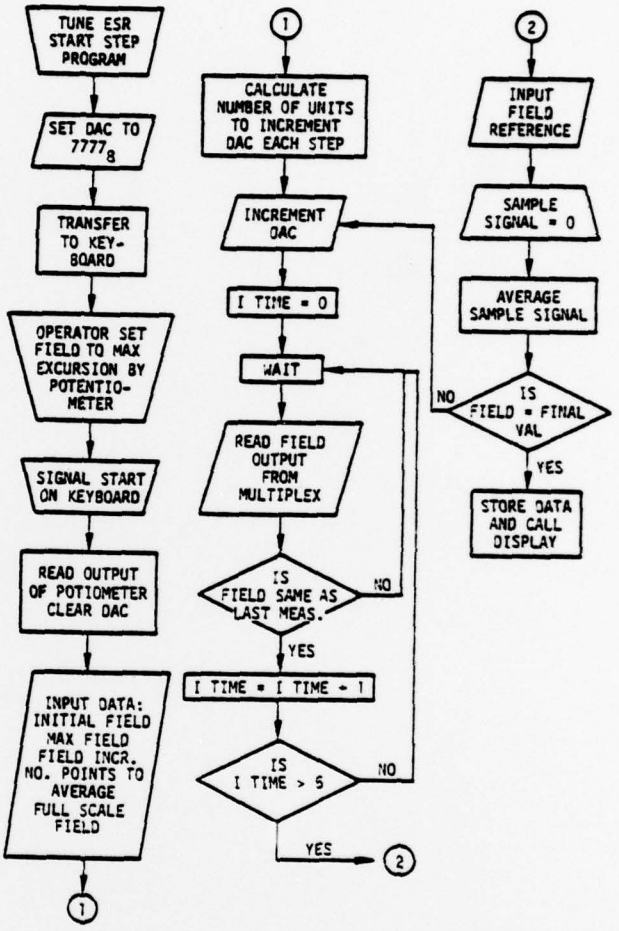

FIG. 2. Abbreviated flow chart of stepped field program.

The computer now loads a value into the DAC that corresponds to the starting field. After a delay of about 1 sec determined by the real-time clock, the field is monitored. When the field output voltages are within a small error after five repetitions, the field value and reference signal values are stored in the computer and the signal is averaged. The averaging process, which is not described in detail in Fig. 2, consists of reading the

sample signal the desired number of times, at intervals equal to the time constant of the filter of the signal channel.

After averaging the signal, the DAC is reset to a value that increases the field by one step. When the field is equal to the final field value, the signal-time or signal-field data are transferred to the disk for permanent storage, and control is transferred to a display program. The display program is straightforward and is written to scale the data for display on an $X-Y$ recorder, or an $X-Y$ storage oscilloscope.

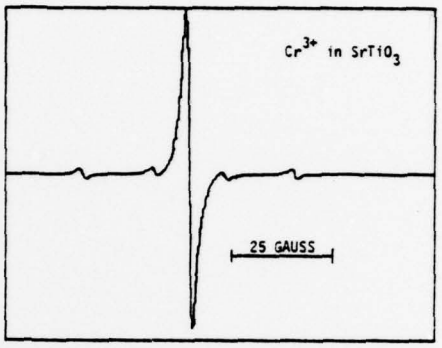

FIG. 3. ESR spectrum of the Cr^{3+} in strontium titanate recorded by the stepped field program, field step is 0.3.

Spectra obtained using computer control of the ESR are shown in Figs. 3–5. Figures 3 and 4 show the ESR spectra of five ppm Cr^{3+} in strontium titanate, and the ESR parameters determined here agree with those obtained by Muller (*27*). The reference signal (not shown) was DPPH. The field increment was 0.3 G and approximately

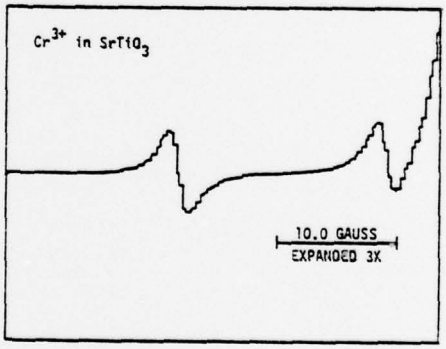

FIG. 4. Expanded view of the low field satellite lines of Cr^{3+} in $SrTiO_3$ shown in Fig. 3.

45 min were required to acquire the data. A 1-sec time constant filter was used on the 100 kHz phase sensitive amplifier, and the signals were added ten times at 1.0-sec intervals. Figure 3 shows the entire spectrum of Cr^{3+} in $SrTiO_3$. The four satellite lines are due to a 9.5% natural abundance of Cr^{53} with a nuclear spin of 3/2. An expansion of the low field side of the spectrum is shown in Fig. 4. The $x-y$ display program

first loads the x-value in one DAC; after a small delay the y-value is loaded in a second DAC. This results in a stepped appearance rather than a straight line between points.

Figure 5 shows a portion of the spectrum of the perylene negative ion (*28*) with the center line being the most intense line (on the right side of the figure) recorded at field increment steps of approximately 0.01 G, and a peak-to-peak modulation amplitude of 0.068 G. The reported hyperfine splittings are 0.450, 3.043 and 3.493 G each for four protons. Normally this spectrum would be expected to exhibit uniformly shaped lines which are not exhibited in Fig. 5. This spectrum was recorded under the same conditions in the conventional manner using a chart recorder. The apparent asymmetry was found to be the result of strong 100-kHz sidebands. The peak-to-peak linewidth of the derivative was about 0.03 G, and consequently, the average value of 0.01 G per step is too small to obtain maximum resolution of the spectrum, and the sidebands distort

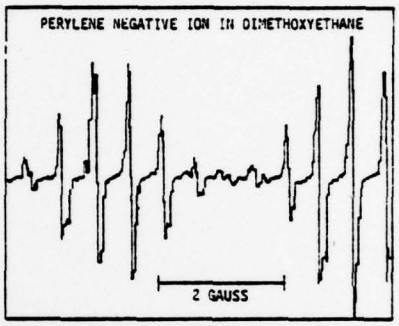

FIG. 5. Spectrum of the perylene negative ion in dimethoxyethane recorded at steps of approximately 0.01 G, and a peak-to-peak modulation amplitude of 0.068.

the apparent lineshape. Smaller steps are possible, but the time required to record a spectrum increases and the maximum range of the spectrum that can be recorded decreases.

A modification to this program was to vary the step size according to whether a signal was observed on the previous accumulation of data. In this case, it was necessary to insure that the noise level after averaging was smaller than the arbitrary input value that is used to assess whether a signal is detected. The maximum field step must be made sufficiently small to avoid missing any absorption peaks. This technique was used successfully in spectra where there are large regions in which no absorption occurs, such as in Fig. 3 or 4, and resulted in a considerable saving of time to record spectra.

This program can be easily modified so that signal-time data and signal-field data can be stored. Changes to the program to accommodate this would be made in the block labeled "Average Sample Signal" of the Flow Chart shown in Fig. 2. An example of a procedure that can be used is the following: (1) Trigger the excitation source. (2) Acquire signal data from the multiplexor or at the desired time intervals. (3) Renew the sample if necessary by activating a solenoid-controlled valve through a monostable multivibrator or a transitor gate. (4) Repeat steps 1–3 the desired number of times. A display program can be called to view the accumulated data, or the experiment can be done for a fixed number of times. (5) Transfer the signal-time data to the disk to minimize

the amount of storage required in core memory. At this point the signal would be stored as a function of time and field, $S(t, H)$. It is straightforward to write a program to print or display $S(t, H)$ vs t at a constant H to permit analysis of the kinetic behavior, or $S(t, H)$ vs H at constant t to observe the change of the spectrum with time.

Sweep Method

The sweep program allows the magnetic field to sweep linearly with time and automatically reverse at the end of the desired excursion, return to the initial field, and start the sweep again. This method does not permit time-dependent data to be determined. The program discussed here is used to accumulate data from a stable paramagnetic sample using the fast sweep available on the magnet. If it is desired to study transient

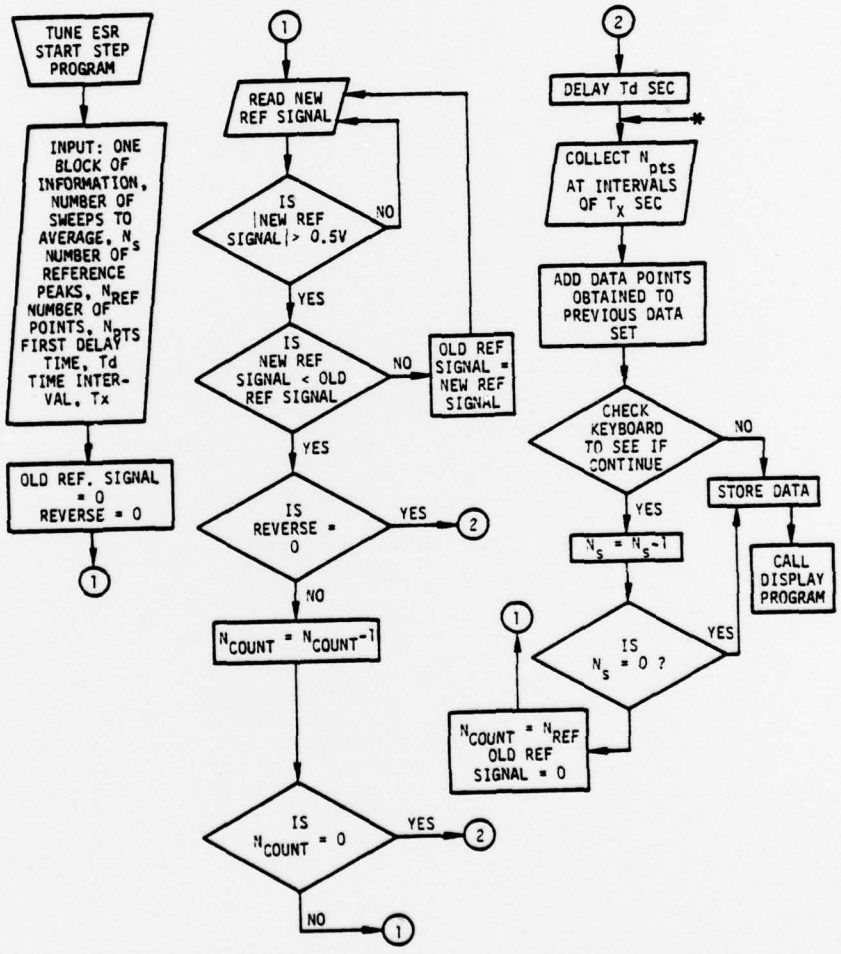

FIG. 6. Abbreviated flow chart of sweep program for data acquisition.

species, this program is easily altered so that an excitation source can be triggered at any time during the sweep. It is also possible to initiate a field sweep in which auxiliary coils are used, although best homogeneity is obtained using the electromagnet sweep facilities. To maximize the speed at which data are acquired, this program was written in a mnemonic assembly language. It is possible to write this program partially in Fortran if a sacrifice of acquisition speed can be tolerated. Either the reference channel or signal channel data can be stored, or, if a factor of two slower acquisition rates than maximum is acceptable, data from the signal and reference channels can be entered at

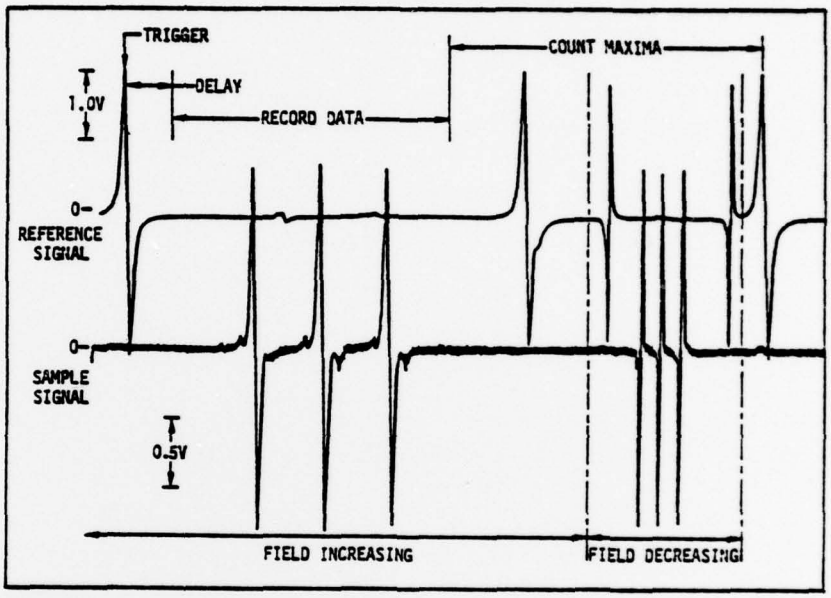

FIG. 7. Diagram of the operation of the sweep program, showing the activity of the computer and the sample and reference signals (see text for description).

alternate times. Although both of these methods have been successful, the program described here averages only the sample signal.

A flow chart of the program is shown in Fig. 6 and a diagram of the activity of the computer as a function of the ESR output is shown on Fig. 7. Initially, the ESR spectrometer is tuned and the computer program is started. At this time the field is stationary and away from any power absorption by the reference material. One block of data (128 words) is allowed for any alpha-numeric input such as parameters which are set by the operator on the ESR spectrometer. The number of sweeps to average (N_s), number of reference peaks (N_{ref}), number of data points (N_{pts}), initial time delay (T_d) and time interval (T_x) are entered by the operator. The significance of these parameters can be understood with the aid of Fig. 7. Generally, the reference absorption does not occur at the same field that the data acquisition should begin. Thus a delay of T_d sec is inserted to eliminate data acquisition over the field in which no absorption by

the sample is expected. The field increment between data points is regulated by controlling the time between data acquisitions (T_x). In order to initiate the delay on the first sweep, the reference signal is read continually. Signals under 0.5 V (or any appropriate value which is suitable considering the reference material used) is ignored to eliminate false triggering. When a decrease in signal from the value of the reference signal measured previously is detected the delay is started. After the data acquisition is completed, the reference signal is again monitored and the reference maxima are counted. This count corresponds to the sum of reference extrema detected while the field is still increasing after the data acquisition is completed and the number of reference maxima observed while the field decreases to a value lower than the field at which the delay is started again (see Fig. 7). When the number of maxima detected is equal to the number which is two times the number of reference absorptions +1, the delay is initiated again. The operator must therefore determine with care the number of reference signals detected over the range of field sweep executed by the magnet. This can be done by sweeping the field at a slower rate than that used during data acquisition. Delays used in the program are determined from the real-time clock. The sweep process is repeated for the number of times desired. When the program is completed, the display routine is called.

Reproducible correspondence between the point number in the set of acquired data and the magnetic field is necessary for high resolution signal averaging. This reproducibility is determined by the reproducibility of the sweep rate of the magnet, the linearity of the sweep, the timing capability of the computer, the analog-to-digital conversion time, and the reproducibility of the trigger to start data acquisition. The reproducibility and linearity of the sweep is determined by the magnet or coils used to sweep the field. Clearly, the electromagnet provides better sweep capabilities than Helmholz coils, as discussed earlier.

Real-time clocks used on most computers are extremely reproducible. The computer will idle in a loop waiting for a clock interrupt so that the random error in the time to begin conversion of data will be of the order of 1 μsec. In most experiments this is not a significant problem. The data-point reading rate is determined by a real-time clock. The clock-interrupt flag is acknowledged by a software priority-polling routine in which the clock is given top priority and the analog-to-digital converter is given second priority. The teletype is the only other peripheral device that can cause an interrupt in this program, and it is given lowest priority. The clock is free running and tissues interrupt pulses at fixed intervals. The program for data collection adds a fixed offset that has an uncertainty of one instruction (1.2 μsec) before the pulse which initiates the sampling and analog to digital conversion. Because this offset is the result of programming time that is constant for each data point, it is not a cumulative effect. The same discussion also applies to monitoring signal-time behavior using the stepped field method.

Two methods of triggering the start of the time delay were used in the program. Both methods regarded signals from the reference channel when they were greater than a certain threshold value, and both methods converted the signal to its absolute value. This threshold value was set depending on the particular reference material. Earlier programs that were used looked for a change of slope from the reference signal to initiate the delay portion of the program. This has the disadvantage that, in the region

of the maximum or minimum peak of the derivative signal, the change of signal with field is small, and therefore even a small amount of random noise can cause entry to the delay portion earlier or later than desired. Even though the reference signal is strong at the small filtering times used, there is significant noise. In the current programs, entry into the delay is started when the reference signal drops below the threshold value after having exceeded the threshold once during each reference peak. By keeping count of the reference peaks, the program insures that this point will be on the rapidly changing portion of the derivative lineshape and not on one of the wings of the signal. If a reference with a peak-to-peak linewidth of 0.10 G is used a sweep rate of 10 kG/min will still insure that at least one point is taken within the threshold limits. The advantage

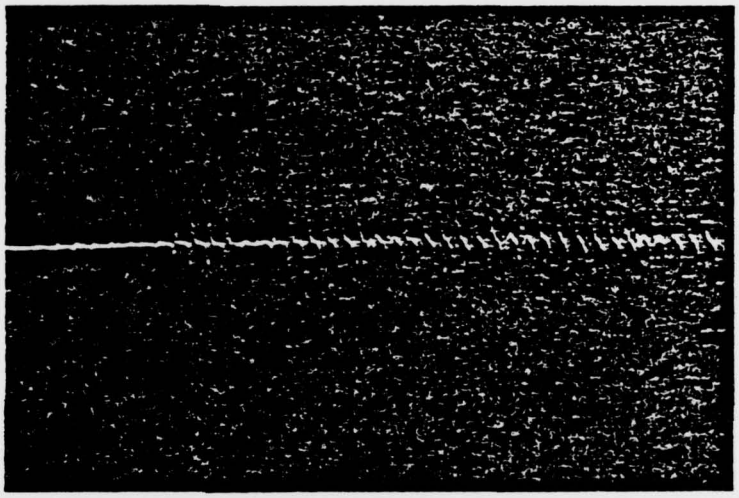

FIG. 8. Spectrum of the perylene anion acquired by the sweep mode. Parameters used are scan rate 3,000 G/min, 1,024 points collected per scan, 0.4 msec delay between points.

of initiating the delay portion of the program in this way is that a reference material with a given linewidth can be used in conjunction with a sample that has a considerably narrower linewidth.

The choice of reference material should depend on the desired sweep range. It is convenient to select a reference in which the desired sweep falls between strong reference absorptions. The references used here are the perylene anion (*28*), Mn^{2+} in Forsterite (*29*, *30*), and a mixture of Mn^{2+} in Forsterite and diluted diphenyl-picryl-hydrazyl. Another property of the reference material should be that the lines that are not used for counting the reference maxima have significantly lower intensity than those that are used. This permits a threshold value to be such that accidental triggering by random noise added to signals close to the threshold value does not occur.

Because filtering is required to obtain stable dc signals on both Hall effect and rotating coil gaussmeters, the field cannot be read directly at fast sweep rates. At slower sweep rates such as described by Newman (*17*) and Gough and Grossman (*18*), where

data are stored on a large computer, it would be a trivial matter to permit values of the magnetic field, reference and sample signals to be read. In some cases an entirely different program would be more suitable. For example, at slow sweep rates, less than about 10 G/min, the field increment could be regulated by taking data when the field output voltage reaches values determined by the computer.

A result of using the sweep method of data acquisition is shown in Fig. 8. Here data are displayed on a storage oscilloscope. The superposition of 256 scans of a dilute solution of perylene anion in dimethoxyethane recorded at 3,000 G/min is shown. The parameters used to acquire these data are: the delay time between the reference absorption and the start of data collection is 1,000 msec; the time between data points is 0.40 msec; and the number of points collected on each sweep is 1024. The rate of data input allows only about 4–5 points per linewidth. Enlargement of a section of Fig. 8 shows that a linewidth of 0.060 G is obtained. This shows reproducibility at high sweep rates.

CONCLUSION

This work shows the application of a laboratory computer for use in controlling and acquiring ESR data in two modes of operation. Computer control offers the advantages of being able to make decisions rapidly concerning the particular experiment, to permit reconstruction or manipulation of stored data for analysis or display, and to store large quantities of permanent data, which are not available on conventional data acquisition instruments. Although general programs were described here, the computer can be programmed to assist specific tasks using ESR. Among these are data acquisition of transient species generated by a variety of different methods, integration and double integration for analyses, and analysis of kinetic data from flow systems. In many cases a minimum change in the electronics of the ESR would be required.

ACKNOWLEDGMENTS

The authors thank Dr. T. P. Graham, Department of Physics, University of Dayton, for a generous sample of Mn^{2+} in Forsterite and Mr. Frank Morin for the use of the single crystal of chromium-doped strontium titanate. Helpful discussions with Dr. Donald Borg, Brookhaven Laboratory, Mr. Jack Gardner, Dr. R. Lee Myers and Dr. George Lauer are acknowledged. This work was supported in part by the Office of Naval Research.

REFERENCES

1. T. J. Bennett, R. C. Smith, T. H. Wilmshurst, *Chem. Commun.* 513 (1967); *J. Phys. E.* **2**, 393 (1969); J. G. Holbrook, T. H. Wilmshurst, and R. R. Simmons, *J. Phys. E.* **5**, 555 (1972).
2. P. W. Atkins, K. A. McLauchlan, and A. F. Simpson, *J. Phys. E.* **3**, 547 (1970).
3. F. W. Firth and D. J. E. Ingram, *J. Sci. Instrum.* **44**, 821 (1967).
4. E. J. Hamilton, D. E. Wood, and G. S. Hammond, *Rev. Sci. Instrum.* **41**, 452 (1970).
5. I. B. Goldberg and A. J. Bard, *J. Phys. Chem.* **75**, 3281 (1971); **78**, 290 (1974); I. B. Goldberg, D. Boyd, R. Hirasawa, and A. J. Bard, *J. Phys. Chem.* **78**, 295 (1974).
6. B. Kastening, B. Gostisa-Mehelcic, and J. Divišek, *Discuss. Faraday Soc.* **56**, 341 (1973).
7. J. K. Dohrmann, F. Gallusser, and H. Wittchen, *Discuss. Faraday Soc.* **56**, 330 (1973).
8. R. W. Fessenden, *J. Chem. Phys.* **58**, 2489 (1973); N. C. Verma and R. W. Fessenden, *J. Chem. Phys.* **58**, 2501 (1973).
9. B. Smaller, E. C. Avery, and J. R. Remko, *J. Chem. Phys.* **55**, 2414 (1971).
10. J. Sohma, T. Komatsu, and Y. Kanada, *Jap. J. Appl. Phys.* **7**, 298 (1968).

11. R. Hirasawa, T. Mukaibo, H. Hasegawa, Y. Kanada, and T. Maruyama, *Rev. Sci. Instrum.* **39,** 935 (1968).
12. E. S. P. Hsi, L. Fabes, and J. R. Bolton, *Rev. Sci. Instrum.* **44,** 197 (1973).
13. J. R. Bolton and J. T. Warden, Publication 39, Photochemistry Unit, Chemistry Department, University of Western Ontario, London, Ontario, Canada.
14. J. E. Beasley, R. L. Anderson, J. P. Dickie, F. R. Dollish, E. C. Tynan and T. F. Yen, *Spectrosc. Lett.* **2,** 149 (1969).
15. K. Ohno and J. Sohma, *Chem. Instrum.* **2,** 121 (1969).
16. C. Klopfenstein, P. Jost, O. H. Griffith, "Computers in Chemical and Biochemical Research" (C. E. Klopfenstein and C. L. Wilkins, Eds.), Vol. 1, p. 175, Academic Press, New York, 1972.
17. L. Newman, "Spectroscopy and Kinetics" (J. S. Mattson, H. B. Mark, and H. C. MacDonald, Eds.), p. 3, Marcel Dekker, New York, 1972.
18. T. E. Gough and F. W. Grossman, *J. Magn. Resonance* **7,** 24 (1972).
19. B. Johnson, T. Kuga, and H. M. Gladney, *IBM J. Res. Develop.* **13,** 36 (1969).
20. J. C. Kertesz, M. B. Wolf, and W. Wolf, *Comput. Prog. Biomed.* **4,** 21 (1974).
21. A. Bauder and R. J. Myers, *J. Mol. Spectrosc.* **27,** 110 (1968).
22. T. O. Seim, T. B. Melo, and S. Pyrdz, *J. Magn. Resonance* **9,** 175 (1973).
23. R. S. Alger, "Electron Paramagnetic Resonance, Techniques and Applications," Chap. 3, Interscience, New York, 1968.
24. I. B. Goldberg, A. J. Lewin, and J. R. Grandall, *Rev. Sci. Instrum.* **45,** 855 (1974).
25. T. Hidaka, *Rev. Sci. Instrum.* **44,** 79 (1973).
26. S. H. Glarum, *Rev. Sci. Instrum.* **44,** 752 (1973).
27. K. A. Muller, *Helv. Phys. Acta* **31,** 173 (1958); "Paramagnetic Resonance" (W. Low, Ed.), p. 17, Academic Press, New York, 1962.
28. J. R. Bolton, *J. Phys. Chem.* **71,** 3702 (1967).
29. G. K. Miner, T. P. Graham, and G. T. Johnston, *Rev. Sci. Instrum.* **43,** 1297 (1972).
30. Values of the g-factor of this Forsterite Sample differ appreciably from that cited in Ref. (*29*). Values obtained from measurements using a proton NMR gaussmeter are $g = 2.00095 \pm 0.00006$ G and $a = 86.75 \pm 0.05$ G.

TECHNICAL REPORT DISTRIBUTION LIST

	No. Copies
Office of Naval Research Arlington, Virginia 22217 Attn: Code 472	2
ONR Branch Office 536 S. Clark Street Chicago, Illinois 60605 Attn: Dr. Jerry Smith	1
ONR New York Area Office 715 Broadway, 5th Floor New York, New York 10003 AttN: Scientific Dept.	1
ONR Branch Office 1030 East Green Street Pasadena, California 91106 Attn: Dr. R. J. Marcus	1
ONR Branch Office One Hallidie Plaza - Suite 601 San Francisco, CA 94102 Attn: Dr. P. A. Miller	1
ONR Branch Office 495 Summer Street Boston, Massachusetts 02210 Attn: Dr. L. H. Peebles	1
The Asst. Secretary of the Navy (R&D) Department of the Navy Room 4E736, Pentagon Washington, D. C. 20350	1
Commander, Naval Air Systems Command Department of the Navy Room 4E736, Pentagon Washington, D. C. 20350	1
Defense Documentation Center Building 5, Cameron Station Alexandria, Virginia 22314	12
U.S. Army Research Office P.O. Box 12211 Research Triangle Park, NC27709 AttN; CRD-AA-IP	1
Naval Ocean Systems Center San Diego, California 92152 Attn: Mr. Joe McCartney	1
Naval Weapons Center China Lake, California 93555 Attn: Head, Chemistry Division	1
Naval Civil Engineering Laboratory Port Hueneme, California 93041 Attn: Mr. W. S. Haynes	1
Professor O. Heinz Department of Physics & Chemistry Naval Postgraduate School Monterey, CA 93940	1
Dr. A. L. Slafkosky Scientific Advisor Commandant of the Marine Corps (Code RD-1) Washington, D.C. 20380	1
Office of Naval Research Arlington, VA 22217 Attn: Dr. Richard S. Miller	1
Dr. M. B. Denton University of Arizona Department of Chemistry Tucson, Arizona 85721	1
Dr. G. S. Wilson University of Arizona Department of Chemistry Tucson, Arizona 85721	1
Dr. R. A. Osteryoung Colorado State University Department of Chemistry Fort Collins, Colorado 80521	1

	No. Copies
Dr. B. R. Kowalski University of Washington Department of Chemistry Seattle, Washington 98105	1
Dr. S. P. Perone Purdue University Department of Chemistry Lafayette, Indiana 47907	1
Dr. E. E. Wells Naval Research Laboratory Code 6160 Washington, D. C. 20375	1
Dr. D. L. Venezky Naval Research Laboratory Code 6130 Washington, D.C. 20375	1
Dr. H. Freiser University of Arizona Department of Chemistry Tuscon, Arizona 85721	1
Dr. Fred Saalfeld Naval Research Laboratory Code 6110 Washington, D.C. 20375	1
Dr. H. Chernoff Massachusetts Institute of Technology Department of Mathematics Cambridge, Massachusetts 02139	1
Dr. K. Wilson University of California, San Diego Department of Chemistry La Jolla, CA 92037	1
Dr. A. Zirino Naval Undersea Center San Diego, CA 92132	1
Dr. John Duffin United States Naval Post Graduate School Monterey, CA 93940	1
Dr. G. M. Hieftje Department of Chemistry Indiana University Bloomington, Indiana 47401	1
Dr. Victor L. Rehn Naval Weapons Center Code 3813 China Lake, CA 93555	1
Dr. Christie G. Enke Michigan State University Department of Chemistry East Lansing, Michigan 48824	1